PHYSICAL REVIEW B VOLUME 31, NUMBER 1 1 JANUARY 1985

# Neutron-diffraction study of the magnetic ordering in $Ni(CH_2CO_2NH_2)_2 \cdot 2H_2O$

O. A. Pringle
*Solid State Division, Oak Ridge National Laboratory, Oak Ridge, Tennessee 37831*

R. Calvo and R. E. Parra
*Centro de Física, Instituto Venezolano de Investigaciones Científicas, Apartado 1827, Caracas 1010A, Venezuela*
(Received 16 July 1984)

The magnetic structure of $Ni(CH_2CO_2NH_2)_2 \cdot 2H_2O$ has been determined by the analysis of neutron-diffraction data from powder and single-crystal samples. $Ni(CH_2CO_2NH_2)_2 \cdot 2H_2O$ orders at a Néel temperature of 0.88 K. The magnetic structure consists of antiferromagnetically coupled layers having a canted ferromagnetic ordering within layers, with a moment of $(2.33 \pm 0.14)\mu_B$ per $Ni^{2+}$ ion. The magnetic unit cell is composed of two crystallographic unit cells, and contains four nickel atoms. The moment direction is not simply related to either crystalline or molecular symmetry axes.

## I. INTRODUCTION

Nickel diglycine dihydrate [$Ni(CH_2CO_2NH_2)_2 \cdot 2H_2O$], hereafter called NiDD, is a metal derivative of the amino acid glycine. NiDD is interesting in that it is a possible metamagnet with a single-ion anisotropy large compared to the magnetic interaction between nickel ions. The compound is also a good model system for metal ions in proteins, and from it one may learn something about electronic properties, magnetic interactions, and electronic paths for superexchange in these macromolecules.

Magnetic susceptibility[1] and specific-heat[2] measurements have previously been reported for NiDD. The specific-heat data indicate a phase transition at 0.88 K and a double Schottky peak due to the zero-field splitting of the $Ni^{2+}$ ions in a low-symmetry environment. The magnetic susceptibility data were obtained from powder and oriented single-crystal samples. At high temperatures the powder susceptibility follows a Curie law with an antiferromagnetic Curie temperature of 2.47 K and a magnetic moment $\mu_{\text{eff}} = 3.19\mu_B$. At low temperatures the magnetic susceptibility data deviate from this behavior, and below 2.2 K the susceptibility decreases with decreasing temperature for every orientation of the magnetic field.

The magnetic susceptibility and specific-heat data were used to construct a model for describing the magnetic properties of NiDD.[1] The $Ni^{2+}$ ions have an effective spin $\vec{S}$ with $S=1$. The single-ion Hamiltonian in a low-symmetry environment, and with an applied magnetic field $\vec{H}$, can be written as

$$\mathcal{H} = D[S_z^2 - S(S+1)/3] + E(S_x^2 - S_y^2) + g\mu_B \vec{H} \cdot \vec{S} , \qquad (1)$$

where $D$ and $E$ give the magnitude of the interaction of the $Ni^{2+}$ ions with the crystal field, $g$ is the gyromagnetic factor, which is assumed to be isotropic, and $\mu_B$ is the Bohr magneton.

From the specific-heat data, taken in zero magnetic field, the values $D = -14.5K$ and $|E| = 1.13$ K, and the phase transition temperature $T_N = 0.88$ K, were determined.[2] The specific-heat data did not allow the determination of the anisotropy axes to which the Hamiltonian of Eq. (1) is referred. The magnetic susceptibility data were compared to a simple molecular-field model similar to the one used by Berger and Friedberg[3] to explain the magnetic susceptibility of $Ni(NO_3)_2 \cdot 2H_2O$, a well-known metamagnet. The predictions of this two-sublattice molecular-field model did not give satisfactory agreement with the data for NiDD.[1] The poor agreement was attributed to the fact that the model did not consider the different orientations of the anisotropy axes for the two $Ni^{2+}$ ions in the crystalline unit cell.

In order to understand the magnetic properties of NiDD we have made neutron-diffraction measurements on both powder and single-crystal NiDD samples at temperatures above and below the magnetic transition temperature. Our measurements reveal a true three-dimensional antiferromagnetic transition at 0.88 K. We have measured the order parameter as a function of temperature below this transition, and we have determined the magnetic structure of NiDD in the ordered phase from the analysis of the magnetic scattering. The magnetic unit cell of NiDD is formed by doubling the crystallographic unit cell along the $a$ axis. The $Ni^{2+}$ ions are arranged in layers parallel to the $bc$ plane, with a canted ferromagnetic structure within layers and an antiferromagnetic coupling between adjacent layers.

## II. CRYSTAL STRUCTURE OF NiDD

The crystal structure of NiDD was originally reported by Stosick,[4] and refined by Freeman and Guss[5] and by Castellano *et al.*[6] NiDD crystallizes in the monoclinic $P2_1/c$ space group, with two NiDD molecules per unit cell. Two glycine residues are bonded to each nickel to form a complex having inversion symmetry around the nickel, as shown in Fig. 1. The two nickel atoms are located at the (0,0,0) and $(0,\frac{1}{2},\frac{1}{2})$ positions in the unit cell. The NiDD molecule centered at $(0,\frac{1}{2},\frac{1}{2})$ is obtained from the NiDD molecule centered at (0,0,0) by a rotation of

 

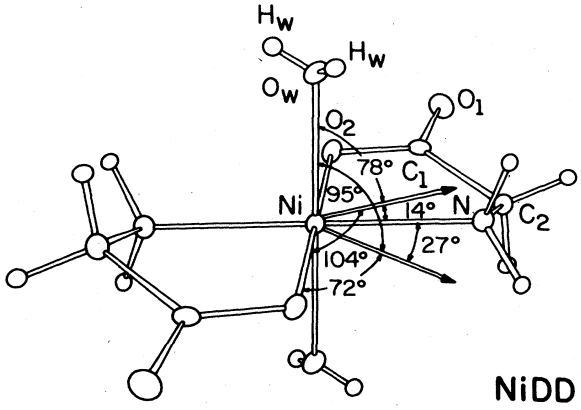


FIG. 1. A molecule of nickel diglycine dihydrate. The arrows represent the $Ni^{2+}$ moment directions as determined by neutron diffraction.

180° around the $b$ axis of the unit cell. The lattice parameters are $a=7.616$ Å, $b=6.601$ Å, $c=9.651$ Å, and $\beta=116.52°$. In this structure the $Ni^{2+}$ ions are arranged in layers parallel to the $bc$ plane. Each $Ni^{2+}$ ion has four nearest neighbors at 5.618 Å and two next-nearest neighbors at 6.601 Å, all within the same layer, while the minimum distance between $Ni^{2+}$ ions in different layers is 7.616 Å.

An orthogonal projection of some of the atoms on or near the $bc$ plane is shown in Fig. 2. We emphasize in this figure the fact that the shortest chemical path between $Ni^{2+}$ ions in this plane contains a hydrogen bond between a water oxygen bonded to one of the nickels and a carbon oxygen bonded to the nearest rotated nickel. From Figs. 1 and 2 it is clear that if the anisotropy energy makes a given orientation of the spin $\vec{S}$ with respect to the molecular axes energetically more favorable, then that orientation will be different with respect to the crystal axes for the different $Ni^{2+}$ ions in the unit cell. Even in the absence of any point symmetry other than the inversion symmetry around the $Ni^{2+}$ ions, one might hypothesize that the direction joining the oxygens of the water molecules in Fig. 1 is the appropriate molecular $z$ anisotropy axis to which the single-ion Hamiltonian of Eq. (1) is referred. As will be discussed later, the interplay between the anisotropy energy and the exchange interactions determines the orientation of the $Ni^{2+}$ moments in the ordered phase.

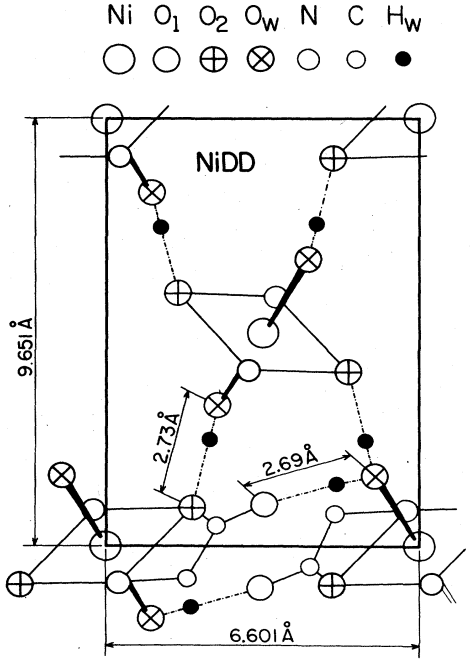


FIG. 2. Orthogonal projection of some of the nickel diglycine dihydrate atoms on or near the $bc$ plane.

## III. EXPERIMENTAL

For our neutron-diffraction measurements we used NiDD synthesized as outlined by Stosick[4] and detailed by Sen *et al.*[7] Single crystals weighing up to 10 mg with dimensions up to $2\times2\times2$ mm$^3$ were obtained by slow evaporation (typically 2 months) at room temperature from a water solution. The material was purified by successive recrystallizations. The resulting NiDD crystals are not hygroscopic and are very stable. We obtained deuterated NiDD powder from small deuterated crystals which had been twice recrystallized in $D_2O$. Our intention in using deuterated samples was to look for differences in superexchange interactions caused by replacement of $H_2O$ by $D_2O$, as well as to minimize the incoherent background scattering from the hydrogen in NiDD. It turned out that the magnetic scattering from the deuterated powder was so weak that we were unable to determine any details of the magnetic structure from it.

We made our neutron-diffraction measurements at the High Flux Isotope Reactor at Oak Ridge National Laboratory using a standard triple-axis spectrometer set for elastic scattering. We used a neutron wavelength of 2.351 Å, with pyrolytic graphite as both a monochromator and a filter to remove higher-order wavelength contamination. Neutron counting times were made versus a monitor counter placed in the reactor beam to account for any small variations in reactor power. The sample was mounted in a $^3$He refrigerator with a low-temperature capability of about 0.4 K. Ge resistance thermometers were used to measure the temperature.

## IV. EXPERIMENTAL RESULTS AND DATA ANALYSIS

### A. Integrated intensity and magnetic structure factor

Before presenting our results, we give expressions for the integrated intensity of a Bragg reflection from a single crystal, and for the structure factor for magnetic neutron scattering from NiDD for a unit cell with space group $P2_1/c$ doubled antiferromagnetically along any of the crystal axes. These expressions will be used in the analysis of our data.

We measure the integrated intensity of an $(hkl)$ reflection by rotating the crystal through the Bragg reflection

position. In the absence of extinction, the integrated intensity for a single crystal completely irradiated by the neutron beam is given by

$$E_{hkl}=KI_0F_{hkl}^2e^{-2W}A_{hkl}/\sin(2\theta)\ , \tag{2}$$

where $\theta$ is the Bragg angle of the $(hkl)$ reflection, $KI_0$ is an instrumental constant, $F_{hkl}$ is the structure factor, $A_{hkl}$ is an absorption correction, and $\exp(-2W)$ is the Debye-Waller factor. We neglect the Debye-Waller factor since we are working at low temperatures, and the absorption is small so we can include it in the instrumental constant. We use the instrumental constant obtained from the Bragg reflections in determining our measured magnetic structure factors.

To calculate the magnetic structure factor, we note that the NiDD crystallographic unit cell contains two $Ni^{2+}$ ions, one located at (0,0,0), which we call site $A$, and the other at $(0,\frac{1}{2},\frac{1}{2})$, which we call site $B$, and that the $Ni^{2+}$ at $B$ is related to the $Ni^{2+}$ at $A$ by a rotation of 180° around the $b$ axis. Let $\vec{\mu}_A$ and $\vec{\mu}_B$ be the atomic magnetic spin vectors at the two sites. Then from symmetry considerations we expect $\vec{\mu}_B$ to be either a rotation by 180° of $\vec{\mu}_A$ around the $b$ axis, or else a rotation of 180° followed by an inversion. The latter case is called an antirotation.

Now consider a magnetic unit cell possibly doubled along each of the crystallographic axes. The structure factor for magnetic neutron scattering is

$$\vec{F}_{hkl}=p(1-\delta_ae^{i\pi h})(1-\delta_be^{i\pi k})(1-\delta_ce^{i\pi l})$$
$$\times[\hat{q}_A+\hat{q}_B\exp i\pi(k/2^{\delta_b}+l/2^{\delta_c})]\ , \tag{3}$$

where $p=(\gamma e^2/2mc^2)\mu f$, $(\gamma e^2/2mc^2)=-0.2695\times10^{-12}$ cm, $\mu$ and $f$ are the magnetic moment and form factor of each $Ni^{2+}$ ion,

$$\delta_{a,b,c}=\begin{cases}1 & \text{if the magnetic unit cell is doubled along } a,b,c\\ 0 & \text{otherwise}\ ,\end{cases}$$

and $(hkl)$ are the indices of the magnetic reflection in terms of the *doubled* unit cell. The magnetic interaction vectors $\hat{q}_A$ and $\hat{q}_B$ are determined from

$$\vec{q}_{A,B}=\hat{k}(\hat{k}\cdot\hat{\mu}_{A,B})-\hat{\mu}_{A,B}\ , \tag{4}$$

where $\hat{k}$ is the scattering vector for the $(hkl)$ reflection. As an example, the structure factor for a magnetic unit cell doubled along the $a$ axis only is

$$\vec{F}_{hkl}=p(1-e^{i\pi h})(\hat{q}_A+\hat{q}_Be^{i\pi(k+l)})\ . \tag{5}$$

Equation (5) gives the selection rule $hkl$: $h=2n+1$ for magnetic reflections for a unit cell doubled along the $a$ axis. Whether the $B$ site is related to $A$ site by a rotation or an antirotation determines the signs of the components of $\hat{\mu}_B$ relative to the signs of the components of $\hat{\mu}_A$.

### B. Deuterated powder sample

We measured diffraction patterns from a powder sample of deuterated NiDD at temperatures of 4.2 and 0.47 K. Deuterated single crystals were not available. Due to the low density of $Ni^{2+}$ ions in NiDD, the magnetic scattering was so weak that only the most intense magnetic reflection was just visible above background in the 0.47-K powder pattern. This reflection could be indexed as $(\frac{1}{2}\,0\,0)$ in terms of the chemical unit cell. The reflection first appeared at a temperature just below 0.9 K, in agreement with the specific-heat measurements.

The power-pattern data thus suggested that NiDD orders antiferromagnetically below 0.9 K with a doubling of the unit cell along the $a$ axis. The absence of other observable magnetic reflections prevented us from drawing any conclusions regarding the ordering in the $bc$ plane.

### C. Single-crystal sample

We made neutron-diffraction measurements on a (nondeuterated) NiDD single crystal using three different sample orientations. These orientations consisted of placing the crystalline $ac$, $ab$, and $bc$ planes in the scattering plane of the neutrons. With these orientations we were able to observe Bragg and magnetic reflections which indexed as $(hk0)$, $(h0l)$, and $(0kl)$. We used the observed magnetic reflections along with Eq. (3) to determine whether the magnetic unit cell was doubled along any of the crystal axes.

The presence of the vacuum and helium gas-handling systems attached to our cryostat limited us to scattering angles less than 65° and limited us to rotating the crystal through an angular range of about 180° around the vertical. Subject to these limitations, we scanned all the Bragg and magnetic reflections we could reach at temperatures above and below the 0.88-K transition temperature. We observed magnetic reflections with the crystalline $ab$ and $ac$ planes in the neutron-scattering plane, and we measured the magnetic order parameter in these two planes. The magnetic susceptibility data for NiDD suggest the possibility of ordering at 2.2 K, so we also looked for scattering at temperatures above 0.88 K which could have been caused by a magnetic transition around 2.2 K.

#### *1. Nuclear Bragg reflections*

We measured the integrated intensities of the Bragg reflections at temperatures above and below the 0.88 K transition temperature. No evidence of magnetic scattering was found at the positions of the Bragg reflections. From the integrated intensities we calculated the instrumental constant $KI_0$. We used the instrumental constant to compare the measured structure factors of our Bragg reflections with structure factors calculated from the NiDD atomic positional coordinates given by Castellano *et al.*[6] The agreement was very good for the more intense reflections and for the reflections at lower scattering angles. The background scattering from our cryostat was high and this problem was aggravated by the open collimation required for the rotating crystal measurement of integrated intensities. Consequently, it was difficult to precisely locate the scattering angles of the weaker reflections. The high background, together with the limited adjustability of the sample arcs once the sample was mounted inside the cryostat, generally resulted in lower

than expected measured intensities for the weaker reflections and for the higher angle reflections.

We made preliminary measurements at room temperature of strong and weak reflections from large and small crystals mounted outside the cryostat. Both strong and weak reflections scaled with crystal size, showing extinction to be negligible. This is supported by the good agreement between the observed and calculated structure factors for the more intense Bragg reflections. We calculate the linear absorption coefficient of NiDD to be only about 0.018 $cm^{-1}$ for 2.4-Å neutrons, so absorption corrections should also be small. We did not correct for absorption in any of our calculations.

### 2. *Magnetic Bragg reflections*

For each crystal orientation, at temperatures above and below the 0.88-K transition we looked for magnetic reflections arising from a doubling of the unit cell along any of the crystallographic axes. We observed no magnetic reflections above 0.88 K. Below 0.88 K we observed a number of magnetic reflections which obeyed the selection rule $hkl$: $h=2n+1$, where the index $h$ corresponds to a unit cell doubled along the $a$ axis. Figure 3 shows the temperature dependence (magnetic order parameter) of one of these reflections, the (100) magnetic reflection. The existence of magnetic reflections with $k$ or $l$ even ruled out a doubling of the unit cell along the $b$ or $c$ axes. All observed extinctions were consistent with a magnetic unit cell doubled along $a$ but not along $b$ or $c$. We conclude that the NiDD unit cell is doubled along the $a$ axis only, and we must use the observed magnetic intensities to determine $\hat{\mu}_A$ and $\hat{\mu}_B$ and whether the two nickel sites are related by a rotation or an antirotation.

To distinguish between the two models (rotation and antirotation), we used Eq. (2) as it applies to magnetic neutron scattering:

$$E_{\text{mag}}=KI_0(V_{\text{nuc}}/V_{\text{mag}})^2F^2_{\text{mag}}/\sin(2\theta_{\text{mag}}) , \tag{6}$$

where $F_{\text{mag}}$ is the magnetic structure factor given by Eq. (5), $KI_0$ is the same instrumental constant as in Eq. (2), $V_{\text{nuc}}$ and $V_{\text{mag}}$ are the volumes of the nuclear and magnetic unit cells, and $2\theta_{\text{mag}}$ and $E_{\text{mag}}$ are the scattering angle and integrated intensity of the magnetic reflection. $\vec{F}_{\text{mag}}$ depends on $\hat{u}_A$, the type of $B$ rotation, the moment on the $Ni^{2+}$ ion, and the $Ni^{2+}$ magnetic form factor. We approximated the form factor using the data of Mook.[8] We approached the problem by observing that Eq. (6) can be rewritten as

$$E_{\text{mag}}\sin(2\theta_{\text{mag}})/F^2_{\text{mag}}=(V_{\text{nuc}}/V_{\text{mag}})^2KI_0 . \tag{7}$$

This expression is valid for each magnetic reflection. The right-hand side of Eq. (7) is a constant and the left-hand side depends on $\hat{\mu}_A$ and $\hat{\mu}_B$.

We determine $\hat{\mu}_A$ and $\hat{\mu}_B$ by carrying out a least-squares fit using our observed intensities and Eq. (7). We assumed that the magnitude of the moment was the same on all nickel sites and treated it as a constant in this calculation. We used for $\hat{\mu}_A$ and $\hat{\mu}_B$ a coordinate system $xyz$, where $\hat{x}=\hat{b}\times\hat{c}$, $\hat{y}=\hat{b}$, and $\hat{z}=\hat{c}$. In this system the $Ni^{2+}$ layers are in the $yz$ plane and the $x$ axis is normal to the layers.

If we choose for $\hat{\mu}_A$ a unit vector making polar and azimuthal angles $\theta$ and $\phi$ with the $xyz$ axes, then $\hat{\mu}_B$ is determined from $\hat{\mu}_A$ and the $B$ rotation. All possible unit vectors $\hat{\mu}_A$ and $\hat{\mu}_B$ can be obtained by varying $\theta$ from 0° to 180° and $\phi$ from 0° to 360°. The best fit of Eq. (7) to our observed intensities occurred for $\theta=59.3°$ and $\phi=158.4°$ with the antirotation model. No fit using the rotation model was capable of giving a reasonable set of calculated structure factors.

From the calculated $\theta$ and $\phi$ for the antirotation model we obtain $\hat{\mu}_A=-0.80\hat{x}+0.32\hat{y}+0.51\hat{z}$ and $\hat{\mu}_B=-0.80\hat{x}-0.32\hat{y}+0.51\hat{z}$. We estimate the polar and azimuthal angles to be accurate to within ±5° and the uncertainties of each of the spin components to be about ±0.1. The arrows in Fig. 1 show these two moment directions referred to one of the NiDD molecules. The moment directions on the remaining two $Ni^{2+}$ ions in the magnetic unit cell are coupled antiferromagnetically to those shown in Fig. 1.

Table I shows the calculated and measured scattering angles and structure factors of our observed magnetic reflections. The measured structure factors are obtained from Eq. (6), while the calculated ones use $\hat{\mu}_A$ and $\hat{\mu}_B$ as given above and the $Ni^{2+}$ moment as determined below

We have repeated these calculations neglecting the reflections having the largest differences between calculated and measured structure factors and weighting the reflections according to their statistical accuracy. In both cases the results do not differ significantly from those given above.

As we have already seen in the case of the Bragg reflections, the discrepancy between observed and calculated magnetic structure factors is greatest for the weaker re-

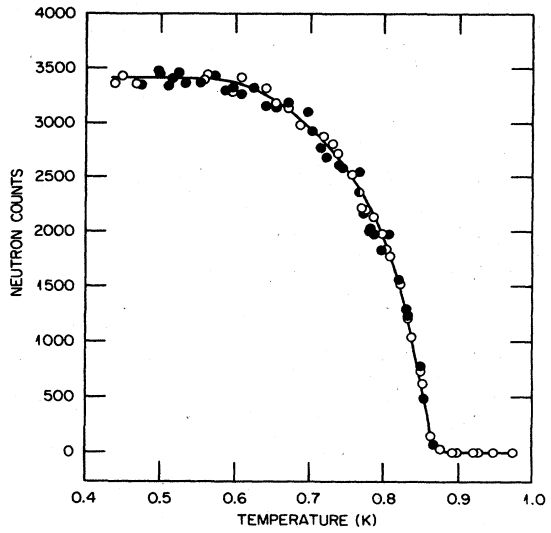


FIG. 3. Temperature dependence of the (100) magnetic reflection of nickel diglycine dihydrate. The open circles represent data taken on cooling, and the solid circles represent data taken on warming. The counting time for each data point was approximately 45 sec.

TABLE I. Comparison of the observed and calculated positions and structure factors of the magnetic reflections for NiDD single crystal. Indices *hkl* are in terms of the magnetic unit cell.

| *hkl* | $2\theta_{obs}$ | $2\theta_{calc}$ | $F^2_{obs}$ | $F^2_{calc}$ |
|---|---|---|---|---|
| 100[a] | 9.4 | 9.90 | 1.88±0.16 | 1.60 |
| 100[b] | 9.6 | 9.90 | 1.43±0.17 | 1.60 |
| $10\bar{1}$ | 14.1 | 14.30 | 0.66±0.09 | 0.61 |
| $\bar{1}0\bar{1}$ | 21.9 | 22.01 | 0.52±0.16 | 0.59 |
| 110 | 22.7 | 22.82 | 0.06±0.03 | 0.11 |
| $30\bar{1}$ | 26.7 | 26.88 | 0.42±0.14 | 0.58 |
| $10\bar{2}$ | 28.3 | 28.50 | 4.88±0.37 | 4.32 |
| 300 | 29.8 | 29.99 | 0.83±0.27 | 1.49 |
| $30\bar{2}$ | 32.4 | 32.47 | 1.13±0.31 | 1.13 |
| $\bar{1}0\bar{2}$ | 37.4 | 37.35 | 4.53±0.44 | 4.86 |
| $\bar{3}0\bar{1}$ | 40.0 | 39.99 | 0.31±0.15 | 0.54 |
| 120 | 43.2 | 42.99 | 1.82±0.20 | 4.58 |
| $\bar{3}0\bar{2}$ | 53.9 | 53.70 | 1.72±0.22 | 3.58 |

[a]Measured with the crystalline *ab* plane in the neutron-scattering plane.
[b]Measured with the crystalline *ac* plane in the neutron-scattering plane.

flections and for the reflections at higher scattering angles. The fact that the observed structure factors are generally less than the calculated ones is once again indicative of the difficulty of precisely locating the weaker reflections. Nevertheless, the doubling of the NiDD unit cell along the *a* axis is firmly established by the observed magnetic reflections and extinctions along with the molecular symmetry at the $Ni^{2+}$ sites. On the other hand, the relatively large uncertainty in the calculated values of $\hat{\mu}_A$ and $\hat{\mu}_B$ is due to the difficulty of obtaining accurate integrated intensity data for the weaker magnetic reflections.

We have also calculated the magnetic moment at each $Ni^{2+}$ site from Eq. (6). In order to avoid underestimating the moment, we used only the reflections for which we believed we measured the full integrated intensity. We chose to omit from the calculation the reflections for which the measured structure factors differed by more than 30% from the calculated structure factors. Accordingly, we calculated the moment using only the (100), $(10\bar{1})$, $(\bar{1}0\bar{1})$, $(30\bar{1})$, $(10\bar{2})$, $(30\bar{2})$, and $(\bar{1}0\bar{2})$ magnetic reflections. We obtained an average $\mu=(2.33\pm0.14)\mu_B$.

### 3. *A 2.2-K transition?*

As we have already noted, the high-temperature magnetic susceptibility data for NiDD follow a Curie law with a Néel temperature of 2.47 K, while the low-temperature data shows a rounded peak around 2.2 K. During our neutron-diffraction measurements we attempted to determine if these effects were due to a magnetic transition around 2.2 K by looking for magnetic scattering from either a commensurate or an incommensurate structure between 2.2 K and 0.88 K.

There was no indication in the positions, intensities, or linewidths of Bragg reflections as the temperature was lowered through 2.2 K that any magnetic transition took place, nor was there any indication of scattering at the positions of the magnetic reflections. Furthermore, scans at temperatures below 2.2 K in reciprocal space between the (100) and (200) reciprocal-lattice points and a network of scans around the (110) reciprocal-lattice point showed no evidence for an incommensurate structure. It is still possible that an incommensurate structure exists but the magnetic scattering was so weak we were unable to detect it, or we looked for it in the wrong region of reciprocal space.

## V. DISCUSSION

An interesting result obtained from the analysis of our neutron-diffraction measurements is that the directions of the $Ni^{2+}$ moments in the ordered phase correspond to neither the molecular nor the crystalline axes of NiDD. The values $D=-14.5$ K and $E=1.13$ K obtained from the specific-heat data[2] indicate a well-defined axial direction for the anisotropy energy, and we have suggested in the crystal structure section that the direction joining the oxygens of the water molecules (see Fig. 1) may correspond to the molecular *z* anisotropy axis.

Since we have no way to identify each of the two molecules in the crystallographic unit cell of NiDD with each of the two moment directions obtained here, we show in Fig. 1 the two possible moment directions referred to one NiDD molecule. The moment directions are in both cases far (about 90°) from the direction joining the waters. The moment direction in the ordered phase of NiDD must be the result of the interplay between the large anisotropy energy (given by *D* and *E*) and the exchange interactions between the canted spins. The exchange interactions must be sufficiently strong to produce large torques which pull the spins away from the anisotropy axis.

The interplay between the exchange and the anisotropy energies also determines the magnitude of the magnetic moment in the ordered phase. The value $\mu=(2.33\pm0.14)\mu_B$ obtained here for the magnetic moment should be compared with the value $\mu_{eff}=3.189\mu_B$ obtained from the magnetic susceptibility data in the paramagnetic phase, which represents the free-ion value. The observed reduction of $\mu$ supports large departures of the spin directions from the single-ion anisotropy energy.

The neutron-diffraction results reported here indicate a magnetic unit cell of NIDD with four Ni atoms. Additional experimental data for NiDD include the magnitude and direction of the magnetic moments, the temperature variation of the order parameter, and the magnetic susceptibility and specific-heat measurements. A molecular-field model intended to explain all the data should be a four-sublattice model which considers the orientations of the axes of the anisotropy energy for the two molecules in the crystallographic unit cell. We understand now why the two-sublattice molecular-field model used previously[1] is not applicable to NiDD. Also, a one-sublattice model such as the one used by McElearney *et al.*[9] to describe $NiCl_2\cdot4H_2O$ would have no physical meaning in our system.

An analysis of the magnetic properties of NiDD using a four-sublattice molecular-field model is being carried out to explain the data obtained at zero magnetic field

(neutron diffraction and specific heat) and the data obtained with an applied magnetic field (magnetic susceptibility). Preliminary results indicate that the transition temperature $T_N=0.88$ K and the magnitude and directions of the magnetic moments in the ordered phase cannot be explained by assuming that the anisotropy $z$ axis is the direction joining the water molecules. In order to complement the present data on the magnetic properties of NiDD, magnetic susceptibility measurements in the millikelvin temperature region are being made[10] and will be reported along with the results of the four-sublattice molecular-field model.

## VI. CONCLUSIONS

We have determined the magnetic structure of NiDD by neutron diffraction. NiDD orders at a Néel temperature of 0.88 K. The ordered phase consists of $Ni^{2+}$ layers coupled antiferromagnetically, with a canted ferromagnetic ordering within layers. The layers lie in planes parallel to the crystalline *bc* plane. This ordering is strongly suggestive of metamagnetism, although we have not made the measurements necessary to establish the metamagnetism of NiDD. The $Ni^{2+}$ ions order with a moment of $(2.32\pm0.14)\mu_B$ per ion, and the moment directions for the two $Ni^{2+}$ ions in the unit cell are given by $\hat{\mu}_A=-0.80\hat{x}+0.32\hat{y}+0.51\hat{z}$ and $\hat{\mu}_B=-0.80\hat{x}-0.32\hat{y}+0.51\hat{z}$, in the $\hat{x}=\hat{b}\times\hat{c}$, $\hat{y}=\hat{b}$, $\hat{z}=\hat{c}$ coordinate system. The moment direction is not simply related to either the molecular or crystalline axes in NiDD, and is most likely the result of the interplay between the anisotropy energy (given by $D$ and $E$) and exchange interactions, represented by the effective-field parameters of the molecular-field model. New magnetic susceptibility measurements in the millikelvin temperature region are being performed for use along with the neutron-diffraction results and a four-sublattice molecular-field model in order to evaluate the exchange interactions in NiDD and to calculate the temperature dependence of the order parameter and the magnetic susceptibility.

## ACKNOWLEDGMENT

This research was sponsored by the Division of Materials Sciences, U. S. Department of Energy, under Contract No. DE-AC05-840R21400 with Martin Marietta Energy Systems, Inc.

[1]R. Calvo, O. R. Nascimento, Z. Fisk, J. Suassuna, S. B. Oseroff, and I. Machin, J. Appl. Phys. **53**, 2674 (1982).

[2]R. Calvo, O. R. Nascimento, M. S. Torikachvili, and M. B. Maple, J. Appl. Phys. **53**, 2671 (1982).

[3]L. Berger and S. A. Friedberg, Phys. Rev. **136**, A158 (1964).

[4]A. J. Stosick, J. Am. Chem. Soc. **67**, 365 (1945).

[5]H. C. Freeman and J. M. Guss, Acta Crystallogr. Sect. B **24**, 1133 (1968).

[6]E. E. Castellano, O. R. Nascimento, and R. Calvo, Acta Crystallogr. Sect. B **38**, 1303 (1982). We have transformed their NiDD positional coordinates to the $P2_1/c$ space group, where it is easier to discuss the magnetic properties of NiDD because the $Ni^{2+}$ ions are arranged in layers.

[7]D. N. Sen, S. Mizushima, C. Curran, and J. V. Quagliano, J. Am. Chem. Soc. **77**, 211 (1955).

[8]H. A. Mook, Phys. Rev. **148**, 495 (1966).

[9]J. N. McElearney, D. B. Losee, S. Merchant, and R. L. Carlin, Phys. Rev. B **7**, 3314 (1973).

[10]O. Symko, M. Novak, R. Calvo, and O. A. Pringle (unpublished).